

Isotopic Transient Kinetic Analysis of CO Hydrogenation on Cu-Modified Ru/SiO₂

Bin Chen and James G. Goodwin, Jr.¹

Chemical and Petroleum Engineering Department, University of Pittsburgh, Pittsburgh, Pennsylvania 15261

Received April 24, 1995; revised September 26, 1995; accepted September 28, 1995

The effect of Cu decoration of Ru/SiO₂ on CO hydrogenation at 1 atm has been studied by isotopic transient kinetics analysis for catalysts having Cu/Ru atomic ratios of 0–0.5. The abundances, coverages, and lifetimes of surface intermediates of the reaction were measured under reaction conditions using isotopic transient kinetic analysis. The effects of temperature and partial pressure of H₂ on these surface reaction parameters were also investigated. Activity distribution analysis showed that there were primarily two kinds of active methanation sites/intermediates (related to pools α and β) as has previously been noted by a number of researchers. Cu preferentially blocked α -type sites. The surface abundance for pool α monotonically decreased with Cu loading while that for pool β only decreased for Cu/Ru > 0.1. Some additional low activity sites for methanation may have been generated with Cu addition due to (a) the spillover of H and CH_x from Ru to Cu permitting reaction to occur on the Cu, or (b) the creation of β -type sites at the Ru–Cu interfaces. The surface abundance of CO measured during the reaction suggests that (a) there was significant spillover of CO from Ru to Cu, and (b) Cu not only blocked the Ru surface but may have possibly caused some reconstruction of it. The surface abundance of intermediates was independent of H₂ partial pressure in the range 18–55 kPa for all the catalysts. © 1996 Academic Press, Inc.

INTRODUCTION

Transition metal catalysts modified by promoters are important in the chemical and petroleum industries (1–11). It is well known that supported Ru is an excellent catalyst for CO hydrogenation while Cu can be considered to be essentially inactive. Since Cu does not alloy with Ru but decorates its surfaces in Ru–Cu catalysts, this bimetallic system offers interesting possibilities to investigate fundamental aspects of catalyst modification, especially surface decoration.

A number of studies of supported Ru–Cu have been reported which can be related to the issue of CO hydroge-

nation (10–11). In the work of Lai and Vickerman (10), the surface structure of Ru with and without Cu present was studied by several UHV techniques. In addition, an infrared study of CO adsorption on Ru–Cu has been reported by Liu *et al.* (11). However, the results of these studies were not able to lead to any conclusions about the nature of the active surface intermediates during reaction. Although not serving as a primary site for CO hydrogenation, Cu may provide a holding area for spillover H (12–14), CO, and CH_x species during reaction due to the intimate contact between Ru and Cu.

The aim of this study was to investigate the effect of Cu on surface abundances and intrinsic activities of the intermediates on Ru/SiO₂ during CO hydrogenation. Isotopic transient kinetic analysis (ITKA) is a unique methodology which is able to provide such information about surface reactions (15–18) and was employed here.

EXPERIMENTAL

Catalyst Preparation

A Ru/SiO₂ base catalyst was prepared using the incipient wetness impregnation method. Ru(NO)(NO₃)₃ (Alfa Chemical), dissolved in distilled water, was impregnated into Cab-O-Sil HS5 fumed silica. The catalyst precursor was dried at 90°C overnight and heated at 1°C/min in flowing hydrogen (Liquid Carbonic, 99.999%) to 300°C and then reduced at this temperature for 8 h. Unless otherwise indicated, all gases (except ¹³CO) were further purified by passing through a molecular sieve and active carbon traps in series. After reduction, the catalyst was washed with boiling distilled water and filtered at least five times in order to remove most of any Cl ions present (19). Ru(NO)(NO₃)₃, which is prepared from RuCl₃, has been found to contain residual Cl. The presence of Cl ions can have a major impact on Ru catalysis (19). After washing, the catalyst was then dried again at 90°C overnight. The catalyst contained 3% ruthenium (by weight). Different amounts of Cu were then added to portions of the Ru/SiO₂ base catalyst using the incipient wetness impreg-

¹ To whom all correspondence should be addressed.

TABLE 1
H₂ Chemisorption on
Ru–Cu/SiO₂ (12)

Catalyst	Irreversible H ₂ uptake ($\mu\text{mol/g}$)		θ_{Ru}^a
	25°C	–196°C	
RuSCu00	54.0	56.4	1.00
RuSCu05	46.7	48.2	0.85
RuSCu10	39.7	30.2	0.54
RuSCu20	43.1	19.5	0.35
RuSCu50	44.2	11.5	0.20

^a Fraction of original surface atoms of Ru not covered by Cu, $\theta_{\text{Ru}} = H_{\text{irrev}}(\text{RuSCu}xx)/H_{\text{irrev}}(\text{RuSCu}00)$ assuming $H_{\text{irrev}}/\text{Ru}_s = 1$ at –196°C.

nation method and aqueous solutions of $\text{Cu}(\text{NO}_3)_2 \cdot 5\text{H}_2\text{O}$ (Alfa Chemical). The Cu-modified catalysts were then re-reduced as mentioned above. The nomenclature used to identify the catalysts is RuSCu xx , where xx indicates the nominal fractional Cu/Ru atomic ratio (RuSCu20 had Cu/Ru = 0.20).

H₂ Chemisorption

Static chemisorption was carried out in a Pyrex glass system. Details of the H₂ chemisorption procedures used are given in Refs. (12, 20). In summary, the catalyst samples were reduced in H₂, degassed for 2 h at 300°C under vacuum, cooled to room temperature, and then further cooled to –196°C. Before introducing H₂, a system pressure $<2 \times 10^{-7}$ Torr was attained. Chemisorption measurements were carried out both at room temperature following the procedure as described in (20) and at –196°C (12). Chemisorption at –196°C was found to accurately determine the amount of surface exposed Ru atoms without the biasing effect of hydrogen spillover onto the Cu surface exhibited at 25°C (12).

Reaction and Isotopic Transient Kinetics Analysis

Reaction and isotopic transients were measured using the system described in Ref. (21). The system had on-line a gas chromatograph (GC) and a mass spectrometer (MS). A Varian 3700 GC with an FID detector and a 6-ft 60–80 mesh Porapak Q column was used. A Leybold-Inficon Auditor-2 MS equipped with a high speed data acquisition system was interfaced to a 386-PC.

Rate measurements of CO hydrogenation were made using 30 to 50 mg of the catalyst loaded in a microreactor. A catalyst sample was re-reduced in a flow of 50 cc/min

TABLE 2
CO Hydrogenation on Ru–Cu^a

Catalyst	Rate ^b [$\mu\text{mol}(\text{CO})/\text{g/s}$]	TOF ^c (10^{-3} s^{-1})	Activation energy (kcal/mol)
RuSCu00	0.64	5.9 ± 0.5	21.7
RuSCu05	0.55	5.7 ± 0.5	22.1
RuSCu10	0.40	6.6 ± 0.5	24.9
RuSCu20	0.27	6.9 ± 0.7	25.5
RuSCu50	0.11	4.8 ± 0.8	27.3

^a Reaction conditions: 240°C, $P_{\text{CO}} = 0.036$ atm, $P_{\text{H}_2} = 0.18$ atm, $P_{\text{total}} = 1.8$ atm, balanced by He.

^b Standard deviation $\leq 5\%$.

^c Determined from $R_{\text{CO}}/H_{\text{irrev},-196^\circ\text{C}}$.

of hydrogen at 400°C for 6 h prior to reaction. This temperature was used since it had been found to be effective for the regeneration of the clean catalyst surface between reaction measurements (see below). However, no difference has been detected for the properties of Ru/SiO₂ using 400°C instead of 300°C for reduction. After reduction, the catalyst bed temperature was lowered to the desired initial reaction temperature in hydrogen. Once the initial reaction temperature had been reached, the feed was switched to the reactant mixture [$P_{\text{CO}} = 1.8$ –5.4 kPa, $P_{\text{H}_2} = 18.3$ –54.9 kPa, $P_{\text{T}} = 182.3$ kPa, with the balance being He (Liquid Carbonic, 99.99%), total flow rate = 100 cc/min], and samples of the products were taken and analyzed after 5 min of reaction. High H₂/CO ratio and initial reaction rate results were used to minimize the effects of carbon deposition and deactivation so that Cu modification of the reaction could be more accurately determined. In all cases, the conversion of CO was less than 5%, and the selectivity to methane was $>88\%$. Small amounts of C₂–C₆ hydrocarbons were also detected. Heat and mass transfer limitations

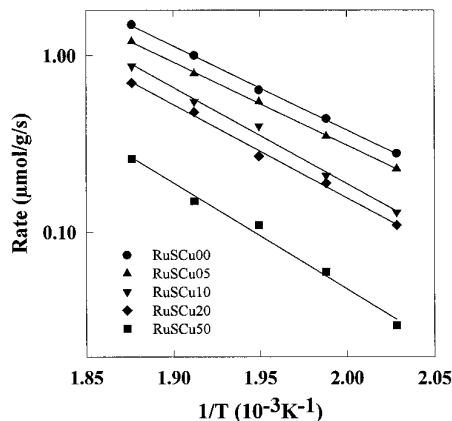


FIG. 1. Arrhenius plots for CO hydrogenation on Ru–Cu catalysts.

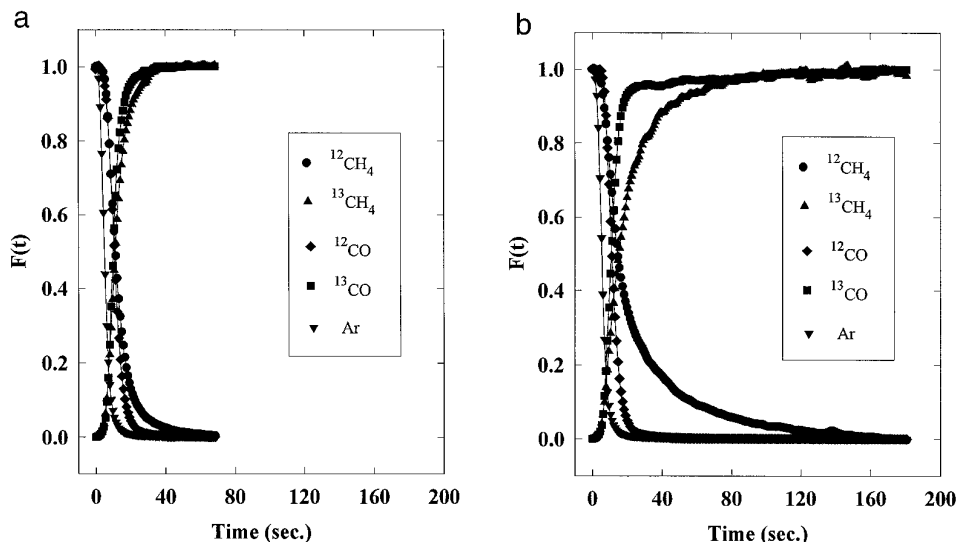


FIG. 2. (a) Normalized isotopic transients during CO hydrogenation on RuSCu00 at 260°C ($H_2/CO = 5$). (b) Normalized isotopic transients during CO hydrogenation on RuSCu50 at 260°C ($H_2/CO = 5$).

were minimized by using low conversions and very high gas space velocities (ca. 600,000 h^{-1}).

Labeled and unlabeled carbon monoxide, ^{13}CO (Isotech, 99.9%) and ^{12}CO (Liquid Carbonic, 99.99%), were used to study the carbon reaction pathway. Switches between the two reactant streams having different isotopically labeled carbon monoxide were able to be made without perturbing the steady operation of the reaction. A trace of argon was present in the ^{12}CO stream in order to permit determination of gas-phase holdup. The isotopic switch was done immediately after 5 min of reaction.

In order to maintain the initial state of the catalyst for reaction at the next temperature, the gas stream was switched to pure H_2 after a total of 10 min of reaction, and the catalyst was re-reduced at 400°C for 2 h before the next measurement. This temperature was used since it was shown to regenerate the catalyst to its original activity after only 2 h of treatment. The measurement at each

temperature was repeated three times. Finally, activity was remeasured at the first reaction temperature studied to make sure that there had been no deactivation during the collection of the temperature dependent data. Reaction and isotopic transient kinetic data were collected at several temperatures between 210 and 260°C. Specific activities were calculated in terms of both the rate of disappearance of CO per gram of catalyst and TOF (s^{-1}).

RESULTS

H_2 Chemisorption on Ru-Cu Catalysts

H_2 chemisorption on Ru-Cu/ SiO_2 was carried out at $-196^\circ C$ in order to prevent hydrogen spillover onto the

TABLE 3

Apparent Reaction Order of H_2

Catalyst	Apparent reaction orders for H_2^a		
	220°C	240°C	260°C
RuSCu00	0.7	0.8	0.6
RuSCu05	0.7	0.8	0.8
RuSCu10	1.0	0.7	0.7
RuSCu20	0.9	0.8	0.7
RuSCu50	0.9	0.7	0.7

^a ± 0.1 .

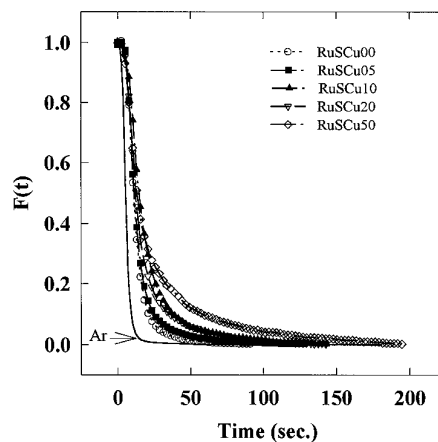


FIG. 3. Normalized isotopic transients of CH_4 during CO hydrogenation on Cu-modified Ru/ SiO_2 at 260°C ($H_2/CO = 5$).

TABLE 4
SSITKA Parameters for CO Hydrogenation on RuSCu00

Temp. (°C)	P_{CO} (kPa)	P_{H_2} (kPa)	R_{CO} ($\mu\text{mol/g/s}$)	TOF (10^{-3} s^{-1})	τ_{CO} (s)	τ_{M} (s)	$k_{\text{M}}(1/\tau_{\text{M}})$ (10^{-3} s^{-1})	N_{CO} ($\mu\text{mol/g}$)	N_{M} ($\mu\text{mol/g}$)	θ_{M}^a
220	3.6	18.3	0.28	2.6	6.0	18.6	54	238	4.6	0.04
240	3.6	18.3	0.64	5.9	6.1	13.0	77	241	7.9	0.07
240	3.6	36.8	1.04	9.6	5.3	7.8	129	207	7.7	0.07
240	3.6	54.9	1.49	13.8	4.9	7.0	143	183	9.8	0.09
260	3.6	18.3	1.49	13.8	6.5	7.8	128	252	11.3	0.10

^a $\theta_{\text{M}} = N_{\text{M}}/\text{Ru}_s$, where Ru_s was determined by irreversible H_2 chemisorption at -196°C .

Cu which occurs at room temperature (12). As shown in Table 1, Cu significantly blocked hydrogen chemisorption sites. Irreversible H_2 chemisorption at room temperature was used to determine that the dispersion of Ru in the base Ru/SiO₂ catalyst (RuSCu00) was 36%. Based on this measurement, the average Ru particle size was calculated to be 2.4 nm. The particle size was assumed not to change with addition of Cu since Cu was impregnated sequentially to different loading on the pre-reduced Ru catalyst. This has been found to be the case for Ru/SiO₂ modified in a similar manner by sequential addition of Cl (19) and for Pd/SiO₂ modified by Li (22). This fact was used to calculate the fraction of Ru surface atoms not covered by Cu, θ_{Ru} (Table 1).

Initial Activity for CO Hydrogenation

(1) *Global reaction rate and TOF.* Table 2 shows that the global reaction rate decreased as the loading of Cu increased. However, TOF did not seem to vary significantly with increasing loading of Cu. This is in agreement with the noted structure insensitivity of this reaction (23). Figure 1 shows the effect of temperature on reaction for all the catalysts. The activation energy increased somewhat with increasing loading of Cu (Table 2).

(2) *Apparent reaction order of H_2 at different temperatures.* Table 3 shows the apparent reaction orders for H_2 .

At 220°C, the hydrogen reaction order seemed to increase slightly with increasing Cu loading. However, at and above 240°C there appeared to be little effect of Cu on this quantity.

Isotopic Transient Analysis of CO Hydrogenation

Isotopic transient analysis was applied in this study in order to investigate in more detail the effect of Cu on surface reaction parameters. Typical normalized transients are shown in Figs. 2a and 2b. Average surface residence times for the carbon in CO and CH₄ are given by the area between the ¹²CO and ¹²CH₄ normalized transients and that of the Ar, which marks the gas-phase holdup. The surface residence times (of CH₄ and of unreacted CO) and reaction rates measured at various temperatures and pressures are summarized in Tables 4–8. As can be seen from these tables, the surface residence time of carbon leading to methane, τ_{M} , increased significantly with increasing loading of Cu. The CH₄ transients collected at 260°C and $\text{H}_2/\text{CO} = 5$ for all the catalysts are displayed in Fig. 3. Under the conditions studied, the Ar transient (measuring gas-phase holdup) was so close to a step input relative to the CH₄ transients that a plug-flow model could be assumed for gas-phase holdup correction (24). This assumption was employed (see later) in the determination of the distribution of intrinsic activity. Surface coverages, N_{CO}

TABLE 5
SSITKA Parameters for CO Hydrogenation on RuSCu05

Temp. (°C)	P_{CO} (kPa)	P_{H_2} (kPa)	R_{CO} ($\mu\text{mol/g/s}$)	TOF (10^{-3} s^{-1})	τ_{CO} (s)	τ_{M} (s)	$k_{\text{M}}(1/\tau_{\text{M}})$ (10^{-3} s^{-1})	N_{CO} ($\mu\text{mol/g}$)	N_{M} ($\mu\text{mol/g}$)	θ_{M}^a
220	3.6	18.3	0.23	2.4	6.1	24.8	40	270	5.7	0.06
240	3.6	18.3	0.55	5.7	6.1	15.2	66	260	8.4	0.09
240	3.6	36.8	0.91	9.4	5.4	10.9	92	239	9.6	0.10
240	3.6	54.9	1.29	13.3	5.3	8.5	118	228	10.6	0.11
260	3.6	18.3	1.20	12.4	5.5	9.7	103	237	11.7	0.12

^a $\theta_{\text{M}} = N_{\text{M}}/\text{Ru}_s$, where Ru_s was determined by irreversible H_2 chemisorption at -196°C .

TABLE 6
SSITKA Parameters for CO Hydrogenation on RuSCu10

Temp. (°C)	P_{CO} (kPa)	P_{H_2} (kPa)	R_{CO} ($\mu\text{mol/g/s}$)	TOF (10^{-3} s^{-1})	τ_{CO} (s)	τ_{M} (s)	$k_{\text{M}}(1/\tau_{\text{M}})$ (10^{-3} s^{-1})	N_{CO} ($\mu\text{mol/g}$)	N_{M} ($\mu\text{mol/g}$)	θ_{M}^a
220	3.6	18.3	0.13	2.2	7.5	35.7	28	297	3.8	0.06
240	3.6	18.3	0.40	6.6	7.4	21.7	46	293	7.8	0.13
240	3.6	36.8	0.61	10.1	6.2	12.8	78	245	7.2	0.12
240	3.6	54.9	0.82	13.6	6.2	11.1	90	250	8.5	0.14
260	3.6	18.3	0.87	14.4	7.8	15.1	66	309	12.4	0.21

^a $\theta_{\text{M}} = N_{\text{M}}/R_{\text{u}_s}$, where R_{u_s} was determined by irreversible H_2 chemisorption at -196°C .

and N_{Methane} , were determined from the respective average surface residence times (30). The fractional coverage of active intermediates for methanation on the exposed Ru surface was found to vary from 0.04 to 0.24 (Tables 4–8) as a function of both temperature and Cu loading. Increasing the temperature from 220 to 260°C caused a factor of 2–3 increase in this quantity regardless of Cu loading. Cu loading, especially for $\text{Cu/Ru} \leq 0.1$, also caused a significant increase.

DISCUSSION

Apparent (Global) Kinetic Parameters during CO Hydrogenation

As shown in Table 2, the TOF did not appear to be effected by Cu loading although the rate of the reaction decreased. This agrees well with most observations that this reaction is structure insensitive. However, TOF (based as it is on hydrogen chemisorption) combines the contributions from both intrinsic activity and coverage of active intermediates. Therefore, one is unable to conclude with any certainty based on TOF results alone that Cu did not have an effect on site activity.

Table 2 shows that the apparent activation energy increased with increasing Cu loading. This is consistent with Lai and Vickerman's (10) results for a similar series of

catalysts. This finding could suggest that there is more than one kind of site involved in the reaction or that reaction on the sites is modified by the Cu. Other results, see below, will identify the former rather than the latter as being the cause.

The results show that Cu did not significantly influence H_2 reaction order under the conditions studied (see Table 3). This suggests that Cu did not affect hydrogenation activity.

The overall CO hydrogenation rate versus surface fraction of Ru exposed at three different temperatures is shown in Fig. 4. Plots such as this have been shown to permit the determination of the site ensemble size for structure sensitive reaction from the slope of the line (25). Figure 4 shows that the data results in straight lines with slopes of approximately 1. Compared with average ensemble sizes of 12 atoms determined for a structure sensitive reaction such as ethane hydrogenolysis (25), this result for CO hydrogenation confirms the structure insensitivity of CO hydrogenation on Ru, i.e., a site of ca. 1 atom which is not affected by the crystallographic plane that it is on.

The Effect of H_2 Partial Pressure on Intrinsic Activity and Surface Abundance of Active Carbon

ITKA is a unique methodology which allows one to decouple the contributions from intrinsic activity and sur-

TABLE 7
SSITKA Parameters for CO Hydrogenation on RuSCu20

Temp. (°C)	P_{CO} (kPa)	P_{H_2} (kPa)	R_{CO} ($\mu\text{mol/g/s}$)	TOF (10^{-3} s^{-1})	τ_{CO} (s)	τ_{M} (s)	$k_{\text{M}}(1/\tau_{\text{M}})$ (10^{-3} s^{-1})	N_{CO} ($\mu\text{mol/g}$)	N_{M} ($\mu\text{mol/g}$)	θ_{M}^a
220	3.6	18.3	0.11	2.8	6.4	36.7	27	221	4.1	0.11
240	3.6	18.3	0.27	6.9	6.9	22.0	46	238	5.9	0.15
240	3.6	36.8	0.48	12.3	6.5	14.5	70	224	6.9	0.18
240	3.6	54.9	0.65	16.6	4.9	11.1	90	169	5.5	0.14
260	3.6	18.3	0.70	17.9	5.3	13.3	75	198	9.3	0.24

^a $\theta_{\text{M}} = N_{\text{M}}/R_{\text{u}_s}$, where R_{u_s} was determined by irreversible H_2 chemisorption at -196°C .

TABLE 8
SSITKA Parameters for CO Hydrogenation on RuSCu50

Temp. (°C)	P_{CO} (kPa)	P_{H_2} (kPa)	R_{CO} ($\mu\text{mol/g/s}$)	TOF (10^{-3} s^{-1})	τ_{CO} (s)	τ_{M} (s)	$k_{\text{M}}(1/\tau_{\text{M}})$ (10^{-3} s^{-1})	N_{CO} ($\mu\text{mol/g}$)	N_{M} ($\mu\text{mol/g}$)	θ_{M}^a
220	3.6	18.3	0.03	—	—	—	—	—	—	—
240	3.6	18.3	0.11	4.8	5.5	37.4	27	198	3.6	0.16
240	3.6	36.6	0.17	7.4	5.5	25.3	40	198	3.8	0.17
240	3.6	54.9	0.23	10.0	5.2	11.5	87	188	2.4	0.10
260	3.6	18.3	0.26	11.3	6.0	19.2	52	216	4.6	0.20

^a $\theta_{\text{M}} = N_{\text{M}}/\text{Ru}_s$, where Ru_s was determined by irreversible H_2 chemisorption at -196°C .

face abundance of intermediates, N_i . Since $R = (1/\tau_i) \times N_i$, the intrinsic activity for a pseudo-first-order reaction is the reciprocal of the residence time, τ_i , of the surface intermediates. Thus, a measure of the intrinsic site activity can be calculated from $1/\tau_i$. In the case of methanation, $k_{\text{M}} = 1/\tau_{\text{M}}$, where k_{M} is the pseudo-first-order rate constant. However, since the surface coverage of hydrogen may also affect the reaction, the reaction may only be approximately first order and $k_{\text{M}} = 1/\tau_{\text{M}} = k'_{\text{M}} \times N_{\text{H}}$, where N_{H} = surface abundance of adsorbed hydrogen and k'_{M} is the “true” intrinsic rate constant (“true” site TOF). Thus, $k_{\text{M}} = 1/\tau_{\text{M}}$ is only a “measure” of the true intrinsic rate constant. However, it provides an excellent measure for comparing rates on a series of catalysts after the contribution due to the concentration of C-containing species has been removed. Unfortunately, the concentration of surface hydrogen during reaction is difficult to measure directly using isotopic transients because of the H_2 - D_2 isotopic effect. However, Fig. 5 shows the change in k_{M} with increasing partial pressure of H_2 under constant partial pressure of CO for the various catalysts. The intrinsic activities of

all the catalysts show similar trends with increasing H_2 pressure. This confirms that k is in fact a function of P_{H_2} , with $k = k'P_{\text{H}_2}^a$ (where $a \approx 0.7$). The similar dependence of k on P_{H_2} for all the catalysts lends support to the conclusion, based on H_2 reaction order, that Cu has little/no effect on hydrogenation on Ru.

Figure 6 presents the surface abundance of methane intermediates, N_{M} , as a function of H_2 pressure. The results suggest that the coverage of surface carbon intermediates is essentially independent of H_2 pressure. This is similar to the results found for a $\text{Ni}/\text{Al}_2\text{O}_3$ catalyst (16).

Based on the above discussion, it can be reasonably assumed that, under the reaction conditions used, H_2 had a similar influence on all the catalysts. Thus, it can be concluded that Cu did not appear to affect the Ru catalyst via a modification of hydrogenation activity.

The Influence of Temperature on Intrinsic Activity and Surface Abundance of Intermediates

Figure 7 shows how the approximate intrinsic activities for methanation varied with temperature for the various

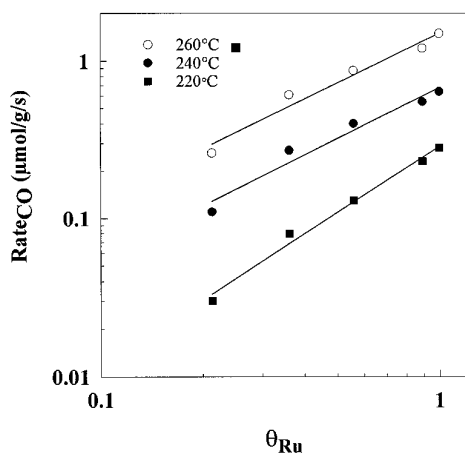


FIG. 4. The overall reaction rate versus the fraction of Ru surface atoms exposed.

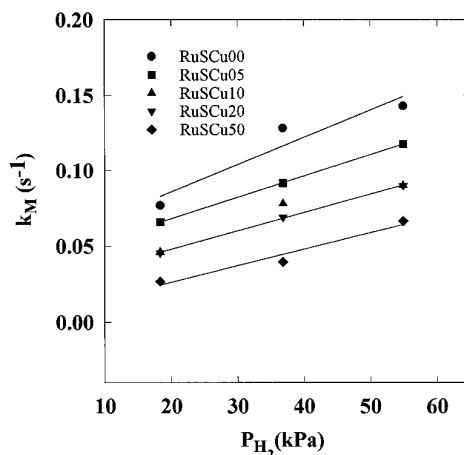


FIG. 5. The intrinsic activity versus partial pressure of H_2 at 240°C .

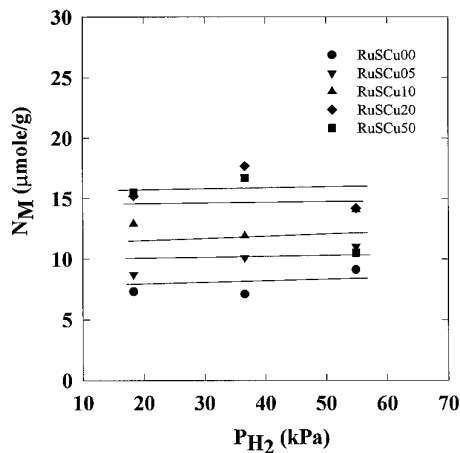


FIG. 6. The abundance of surface CH_4 intermediates versus partial pressure of H_2 at 240°C .

catalysts. The results suggest that the apparent intrinsic activation energies of the catalysts were similar. As can be seen in Fig. 8, an increase in the reaction temperature brought about a significant increase in the surface abundance of intermediates.

CO Adsorption during Reaction

As discussed in the previous study of H_2 chemisorption on Ru-Cu (12), Cu blocks H chemisorption sites on a one-to-one basis initially. Highly dispersed two-dimensional Cu islands are formed for low loadings of Cu. However, as more Cu is added to the Ru ($\text{Cu}/\text{Ru} > 0.2$), three-dimensional Cu structures are able to form before coverage of Ru by Cu is complete (12). In the case of CO chemisorption, the surface abundance of CO (N_{CO}) during reaction at 260°C measured by ITKA shows that N_{CO} went through

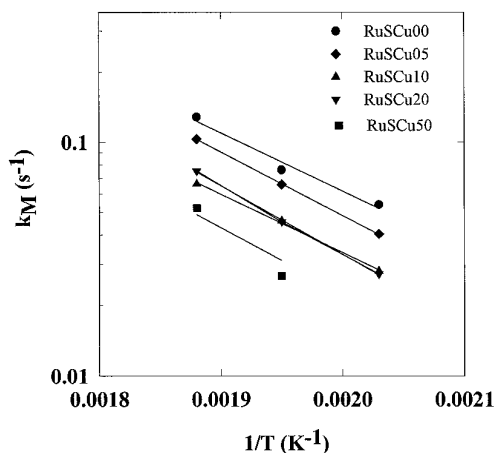


FIG. 7. The intrinsic activity versus temperature ($\text{H}_2/\text{CO} = 5$).

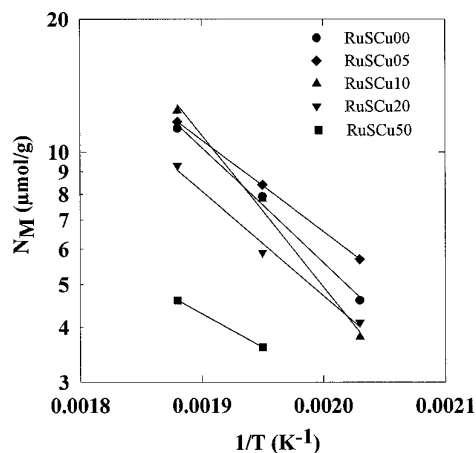


FIG. 8. The surface abundance of CH_4 intermediates versus temperature ($\text{H}_2/\text{CO} = 5$).

a maximum as more Cu was added to the Ru (Fig. 9). This can be explained by two possible ways. Although the Ru surface was partially covered by Cu, CO that initially adsorbed on Ru may have been able to spillover to Cu due to the intimate contact between Ru and Cu. Such an explanation would not, however, account satisfactorily for why there was an increase in the amount of CO chemisorbed for low Cu loadings, even considering the variations in N_{M} .

A more logical explanation may lie in a change in the Ru surface structure as a result of Cu decoration. CO chemisorption on highly dispersed Ru is a function of metal particle size, i.e., coordination number of the surface atoms (26). The CO/H ratio has been found to exceed 1 for Ru catalysts having an average particle diameter, $d_{\text{Ru}} < 3$ nm. In this study, $d_{\text{Ru}} \approx 2.4$ nm. The CO/H chemisorption ratio for the Cu-modified catalysts, determined using $\{N_{\text{CO}}(\text{measured during reaction at } 260^\circ\text{C})/\text{H}_{-196}(\text{irreversible H chemisorption at } -196^\circ\text{C})\}$, increased with the fraction of

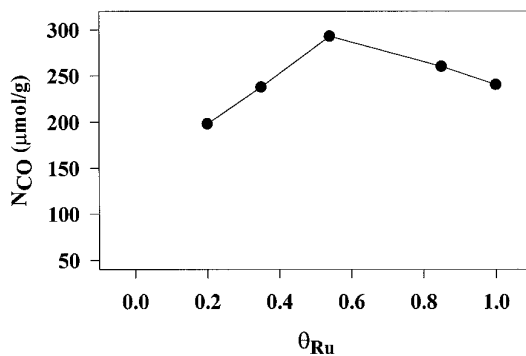


FIG. 9. Surface abundance of CO during the reaction at 260°C vs. the fraction of Ru surface atoms exposed.

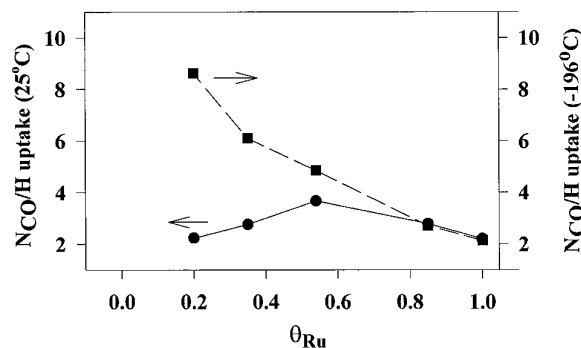


FIG. 10. The ratios of surface abundance of CO during the reaction at 260°C to irreversible hydrogen uptake at 25° and at -196°C vs the fraction of Ru surface atoms exposed.

Ru surface atoms covered by Cu (Fig. 10). On the Cu-free Ru surface ($d_{\text{Ru}} \approx 2.4$ nm in this study), the CO/H ratio was found to be 2.3, which is very similar to what was found using CO and H₂ chemisorption at 25°C for 5 wt% Ru/SiO₂ ($d_{\text{Ru}} = 2.5$ nm) (26). However, N_{CO}/H_{-196} was 8.6 for the Ru surface that was 80% covered by Cu. The maximum possible CO/H ratio should be not greater than 4–5 for the highest dispersed Ru (26). Thus, some of the CO obviously spilled over to or adsorbed on the Cu surface sites. Figure 10 also shows a plot of $[N_{\text{CO}} (@260^\circ\text{C})/H_{25}] \cdot H_{25}$, the irreversible hydrogen chemisorption at 25°C for RuScu00, can be used as an *estimate* of the total number of available Ru and Cu surface sites for adsorption. One sees that N_{CO}/H_{25} passes through a maximum of 3.9 for $\theta_{\text{Ru}} = 0.54$ (Cu/Ru = 0.1). Such a result could be due to a reconstruction of the Ru surface (creation of defect sites) as a result of the presence of Cu yielding CO chemisorption sites with low coordination numbers. Such a reconstruction of a surface in the presence of an adatom has been proposed to be necessary in order to minimize the surface free energy of the system (27). Thus, it is likely that both CO spillover to or adsorption on the Cu surface during reaction and some structural roughening of the exposed Ru surface caused by the presence of Cu may have occurred.

Surface Reaction Kinetics and the Distribution of Site Activities

As shown previously, the fraction of Ru surface atoms exposed decreased monotonically with increasing Cu loading. Figure 11 illustrates clearly how the approximate intrinsic activity also decreased with an increase in Cu coverage (decrease in the fraction of Ru surface atoms exposed). Figure 12 shows the variation in surface coverage of methane intermediates with fraction of Ru surface atoms exposed. Contrary to k_M , the surface abundance of active intermediates did not decrease with the addition of small amounts of Cu, which suggests that Cu did not block any

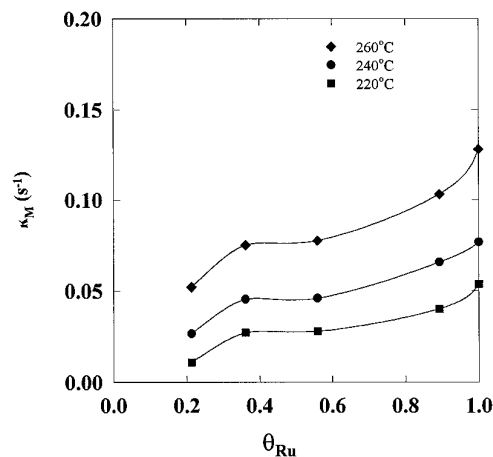


FIG. 11. The intrinsic activity versus the fraction of Ru surface atoms exposed.

active Ru sites at these low loadings. N_M passed through, at best, a slight maximum with increasing loading of Cu before decreasing rapidly (Fig. 12). This is similar to the variation in N_{CO} with Cu loading. These results could be due to reconstruction of the Ru surface caused by Cu, although the reverse spillover of active carbon intermediates from Cu to Ru can not be ruled out as a cause.

The analysis of the distribution of intrinsic activity based on the T-F method developed by Hoost and Goodwin (28) provides a means to explore the effect of catalyst modification on active site heterogeneity. As can be seen from Fig. 13, the activity distribution function, $f(k_M)$, changed significantly with Cu loading. Table 9 summarizes the peak positions and their fraction of the total active intermediates. As can be seen from Table 9 and Fig. 13, the fraction of the most active intermediates (corresponding to pool α) monotonically decreased with increasing Cu loading. However, the position of the two peaks in $f(k_M)$ vs k_M did not change significantly, suggesting that Cu blocked

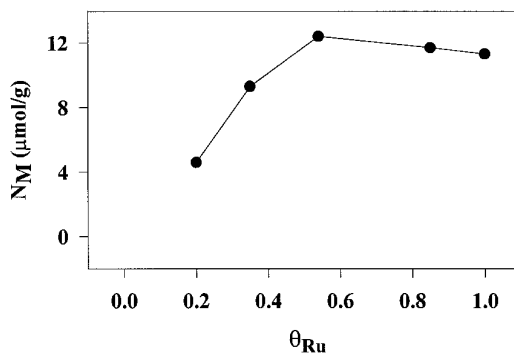


FIG. 12. The surface abundance of active CH₄ intermediates at 260°C vs the fraction of Ru surface atoms exposed.

TABLE 9
Summary of Distribution of the Active Sites By Using the T–F Method

Catalyst	$k_\alpha(\text{s}^{-1})^a$	$k_\beta(\text{s}^{-1})^a$	x_α^b	x_β^b	$N_{M\alpha}$ ($\mu\text{mol/g}$)	$N_{M\beta}$ ($\mu\text{mol/g}$)
RuSCu00	0.141	0.047	0.82	0.18	9.27	2.03
RuSCu05	0.123	0.028	0.77	0.23	9.01	2.69
RuSCu10	0.094	0.038	0.49	0.51	6.08	6.32
RuSCu20	0.119	0.037	0.35	0.65	3.26	6.05
RuSCu50	0.129	0.022	0.21	0.79	0.97	3.63

^a k_α , k_β refer to the value of k at the peaks of $f(k)$ vs k .

^b x_α , x_β indicate the fraction of the active intermediates in pools α and β .

preferentially the most active sites without modifying the properties of any sites. The relative contribution of the sites/intermediates to the reaction rate can be obtained by multiplying $f(k_M)$, the activity distribution function by $(k_M N_M)$ (28). Figure 14 shows the contribution of the various active sites to the reaction rate. With increasing Cu loading, the contribution from pool α monotonically decreased while the contribution from pool β went through a maximum. This behavior was mainly due to the fact that the surface abundance of active carbon for methane formation in pool α , $N_{M\alpha}$, monotonically decreased while that for pool β , $N_{M\beta}$, went through a maximum (Table 9).

It is well known that Cu is much less active for CO hydrogenation under the conditions studied than Ru. However, as shown in Fig. 12, the surface abundance of active intermediates did not decrease monotonically with Cu addition. Since $N_{M\alpha}$ monotonically decreases while $N_{M\beta}$ goes

through a maximum for $\theta_{\text{Ru}} = 0.54$ ($\text{Cu/Ru} = 0.1$) (Fig. 15), it could be suggested that Cu addition resulted in additional low activity sites for methanation. Such additional sites could possibly be due to (a) the spillover of H and CH_x from Ru to Cu, permitting reaction on the Cu, or (b) the creation of β -type sites at the Ru–Cu interfaces (29).

CONCLUSIONS

Ru is an excellent catalyst for CO hydrogenation while Cu can be considered to be essentially inactive. Since Cu does not alloy with Ru but decorates its surface in Ru–Cu catalysts, this bimetallic system offers interesting possibilities for studying fundamental aspects of surface decoration. While TOF for CO hydrogenation remained relatively constant with the addition of Cu, the overall rate decreased

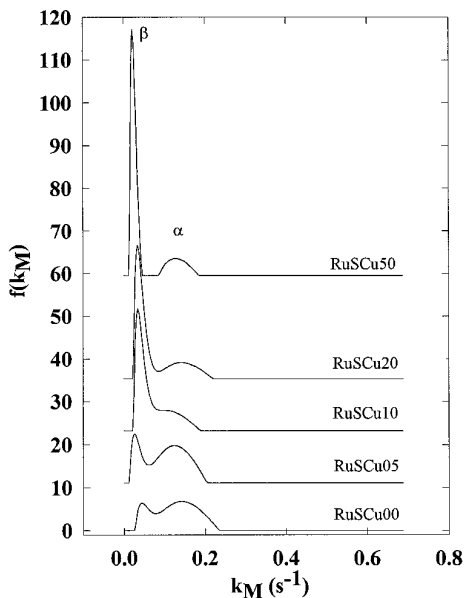


FIG. 13. The distribution of activity.

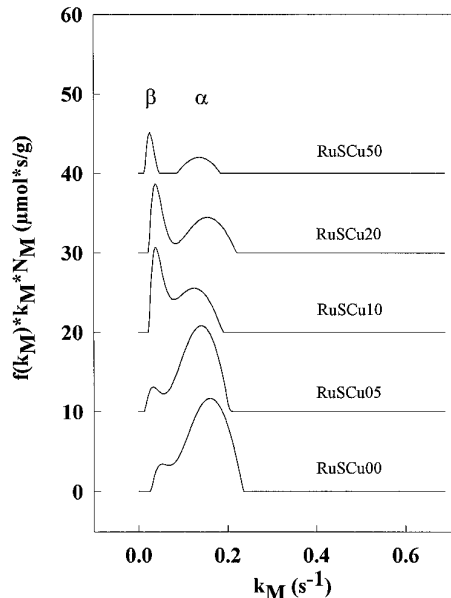


FIG. 14. The contribution of active sites to the reaction rates.

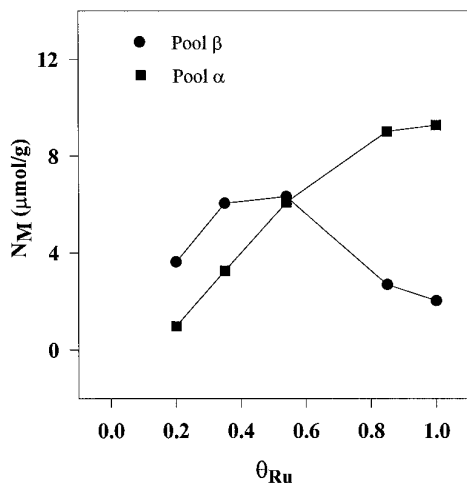


FIG. 15. The surface abundance of active CH_4 intermediates in pool α and β at 260°C vs the fraction of Ru surface atoms exposed.

significantly. However, a measure of intrinsic activity ($k_M = 1/\tau_M$) decreased nonlinearly upon adding Cu, suggesting that the Cu distribution on the Ru surface was not homogeneous.

Analysis of the activity distribution function, $f(k)$, indicated that there were primarily two kinds of active methanation sites/intermediates (α and β). Cu preferentially blocked α -type sites so that the surface abundance for pool α monotonically decreased with Cu loading while that for pool β only decreased for $\text{Cu}/\text{Ru} > 0.1$. Additional low activity sites for methanation may have been created by Cu addition due to (a) the spillover of H and CH_x from Ru to Cu, permitting reaction on the Cu, or (b) the creation of β -type sites at the Ru–Cu interfaces. Cu addition did not, however, seem to have any influence on the effect of hydrogen on reaction.

The surface abundance of CO measured during the reaction indicates that there was significant spillover of CO from Ru to Cu and suggests that Cu not only blocked the Ru surface but may have possibly caused some reconstruction of it.

ACKNOWLEDGMENT

This work was funded by the National Science Foundation (Grant CTS-9102960).

REFERENCES

- Vannice, M. A., *Catal. Rev. Sci. Eng.* **14**(2), 153 (1976).
- Iglesia, E., Soled, S. L., Fiato, S., and Via, H. V., *J. Catal.* **143**, 345 (1993).
- Iglesia, E., Soled, S. L., and Fiato, R. C., *J. Catal.* **137**, 212 (1992).
- Vada, S., Chen, B., and Goodwin, J. G., Jr., *J. Catal.* **153**, 224 (1995).
- Freeley, O. C., and Sachtler, W. M. H., *Appl. Catal.* **75**, 93 (1991).
- Krishna, K. R., and Bell, A. T., *J. Catal.* **130**, 597 (1991).
- Krishna, K. R., and Bell, A. T., *J. Catal.* **139**, 104 (1993).
- Yokomizo, G. H., Louis, C., and Bell, A. T., *J. Catal.* **120**, 1 (1989).
- Yokomizo, G. H., Louis, C., and Bell, A. T., *J. Catal.* **120**, 15 (1989).
- Lai, S. Y., and Vickerman, J. C., *J. Catal.* **90**, 337 (1984).
- Liu, R., Tesche, B., and Knozinger, H., *J. Catal.* **129**, 403 (1991).
- Chen, B., and Goodwin, J. G., Jr., *J. Catal.* **148**, 409 (1994).
- Goodman, D. W., and Peden, C. H. F., *J. Catal.* **95**, 321 (1985).
- Wu, X., Gerstein, B. C., and King, T. S., *J. Catal.* **118**, 271 (1990).
- Biloen, P., Helle, J. N., van den Berg, F. G. A., and Sachtler, W. M. H., *J. Catal.* **80**, 450 (1983).
- Biloen, P., *J. Mol. Catal.* **21**, 17 (1983).
- Yang, C. H., Soong, Y., and Biloen, P., "Proceedings, 8th International Congress on Catalysis, Berlin, 1984," Vol. 2, p. 2. Dechema, Frankfurt-am-Main, 1984.
- Stockwell, D. M., and Bennett, C. O., *J. Catal.* **110**, 354 (1988).
- Iyagba, E. T., Hoost, T. E., and Nwalor, J. U., and Goodwin, J. G., Jr., *J. Catal.* **123**, 1 (1990).
- Goodwin, J. G., Jr., *J. Catal.* **68**, 227 (1981).
- Chen, B., and Goodwin, J. G., Jr., *J. Catal.* **154**, 1 (1995).
- Kazi, A. M., Chen, Bin, Goodwin, J. G., Jr., Marcelin, G., Baker, T., and Rodriguez, N. M., *J. Catal.* **157**, 1 (1995).
- Kelly, R. D., and Goodman, D. W., *Surf. Sci.* **123**, L743 (1982).
- Shannon, S., unpublished results.
- Martin, G. A., *Catal. Rev. Sci. Eng.* **42**, 157 (1974).
- Yang, C. H., and Goodwin, J. G., Jr., *React. Kinet. Catal. Lett.* **20**, 13 (1982).
- Estrup, P. J., in "Chemistry and Physics of Solid Surfaces V" (R. Vanselow and R. Howe, Eds.), pp. 205–230. Springer-Verlag, Berlin, 1984.
- Hoost, E. T., and Goodwin, J. G., Jr., *J. Catal.* **134**, 678 (1992).
- Okuhara, T., Jin, T., Zhou, Y., and White, J. M., *J. Phys. Chem.* **92**, 4141 (1988).
- Shannon, S. L., and Goodwin, J. G., Jr., *Chem. Rev.* **95**, 677 (1995).